The impact of 3D models on positive surgical margins after robot-assisted radical prostatectomy

THE IMPACT OF 3D MODELS ON POSITIVE SURGICAL MARGINS AFTER ROBOT ASSISTED RADICAL PROSTATECTOMY

[1-,3]Enrico Checcucci, [3]Angela Pecoraro, [3]Daniele Amparore, [3]Sabrina De Cillis, [3]Stefano Granato, [3]Gabriele Volpi, [3]Michele Sica, [3]Paolo Verri, [3]Alberto Piana, [4]Pietro Piazzolla, [3]Matteo Manfredi, [4]Enrico Vezzetti, [5]Michele Di Dio, [3§]Cristian Fiori, [3§]Francesco Porpiglia

on behalf of the Uro-technology and SoMe Working Group of the Young Academic Urologists Working Party of the European Association of Urology

[1]Department of Surgery, Candiolo Cancer Institute, FPO-IRCCS, Candiolo, Turin, Italy

[2]Uro-technology and SoMe Working Group of the Young Academic Urologists (YAU) Working Party of the European Association of Urology (EAU), Arnhem, The Netherlands

[3] Department of Oncology, Division of Urology, University of Turin, San Luigi Gonzaga Hospital, Orbassano (Turin), Italy

[4]Department of Management and Production Engineer, Polytechnic University of Turin, Italy

[5]Division of Urology, Department of Surgery, SS Annunziata Hospital, Cosenza, Italy.

[§]These authors contributed equally to senior authorship

Corresponding author:

Enrico Checcucci, MD

Department of Surgery, Candiolo Cancer Institute, FPO-IRCCS

Strada Provinciale 142, km 3,95 10060 Candiolo, Turin – Italy

Email address: checcu.e@hotmail.it

Key words: *Prostate cancer, Augmented Reality, Surgical Margins, 3D modelling, Robotic Surgery*

Word Count (Excl abs)*:* 2495

Abstract word count: 249

ABSTRACT

Purpose: to evaluate the role of 3D models on positive surgical margin rate (PSM) rate in patients who underwent robot-assisted radical prostatectomy (RARP) compared to a no-3D control group. Secondarily, we evaluated the postoperative functional and oncological outcomes.

Methods: prospective study enrolling patients with localized prostate cancer (PCa) undergoing RARP with mp-MRI based 3D model reconstruction, displayed in a cognitive or augmented reality (AR) fashion, at our Centre from 01/2016 to 01/2020. A control no-3D group was extracted from the last two years of our Institutional RARP database. PSMr between the two groups was evaluated and multivariable linear regression (MLR) models were applied. Finally, Kaplan-Meier estimator was used to calculate biochemical recurrence (BCR) at 12 months after the intervention.

Results: 160 patients were enrolled in the 3D Group, whilst 640 were selected for the Control Group. A more conservative NS approach was registered in the 3D Group (full NS 20.6% vs 12.7%; intermediate NS 38.1% vs 38.0%; standard NS 41.2% vs 49.2%; p= 0.02). 3D Group patients had lower PSM rates (25 vs. 35.1%, p=0.01). At MLR models, the availability of 3D technology (p= 0.005) and the absence of extracapsular extension (ECE, p=0.004) at mpMRI were independent predictors of lower PSMr. Moreover, 3D model represented a significant protective factor for PSM in patients with ECE or pT3 disease.

Conclusions: The availability of 3D models during the intervention allows to modulate the NS approach, limiting the occurrence of PSM, especially in patients with ECE at mpMRI or pT3 PCa.

1. INTRODUCTION

In current days, precision prostate cancer (PCa) surgery moves in a delicate balance between oncological and functional outcomes [1].

A relevant risk factor for biochemical recurrence (BCR) after RARP is represented by positive surgical margins (PSM). In fact, the nerve sparing (NS) phase represents the most delicate step of the procedure in this context. Recently published data state that the postoperative PSMr is 5-30% for organ confined PCa and 17-65% for locally advanced PCa [2].

Aiming to reduce the occurrence of this unwanted event, multiple techniques were introduced over the last years [1] such as neurovascular structure adjacent frozen section examination (NeuroSAFE) [3] or confocal laser endomicroscopy [4]. Among them, novel high-definition three-dimensional (3D) models (HA3D^{TM}) represent an innovative solution. These are created based on multiparametric magnetic resonance imaging (mpMRI), able to identify lesion's location and its relationship with the prostate capsule [5]. Such information offer to the surgeon an enhanced spatial visualization of the organ and of the disease.

Several pilot studies already demonstrated the utility of this technology in surgical planning [6] or for surgical navigation [7,8], and, regardless of the ways of application (physical or virtual), it seems to help the surgeon to have a better comprehension of the disease compared to standard 2D images [9].

The aim of this study was to evaluate if the intraoperative availability of HA3D^{TM} models can have an impact on PSMr, then functional and oncological outcomes were analyzed.

2. MATERIALS AND METHODS

2.1 Study population

Patients with prostate cancer (clinical stages cT1–3, cN0, cM0) who underwent robot-assisted radical prostatectomy (RARP) with 3D model reconstruction at our Centre were prospectively enrolled in our study from January 2016 to January 2020. The study was conducted in accordance with the Declaration of Helsinki, and informed consent was obtained from the patients.
In all cases, prostate cancer diagnosis was based on a positive target biopsy of the index lesion [10] and preoperative staging was performed according to EAU guidelines. Exclusion criteria were any contraindications to RARP and absence of a detectable lesion at the preoperative mpMRI.

2.2 mpMRI images and HA3D^{TM} models' reconstruction

Preoperative assessment included a mpMRI following a dedicated protocol, as previously described [8], with 1.5T or 3T and with or without endorectal coil depending on the MRI machine characteristics. All the mpMRI were performed by dedicated uro-radiologists that already walked their learning curve. Briefly, 3D imaging realization started from the acquisition of DICOM images and their processing with a dedicated software, authorized for medical use by MEDICS Srl (www.medics3d.com). The first step consisted in an automatic volume rendering, followed by a process called "segmentation", aimed to define and isolate pixels included in regions or objects of interest (ROI/OOI). In some cases, the software was not able to correctly identify and depict the different features, so the process needed to be performed manually by an expert urologist together with a bioengineer. Once this phase was completed, the project was exported and saved in .stl format (Figure 1a).
The completed virtual 3D model could then be displayed in a "cognitive" manner on a screen (e.g., iPad or laptop) where it could be zoomed, tilted, rotated and translated according to operator's needs.
Moreover, thanks to bioengineers support, augmented reality (AR) RARP was performed thanks to a real-time intraoperative overlapping of the 3D model inside the robotic console.

2.3 **3D Cognitive or Augmented-Reality RARP**

All the procedures were performed according to our total anatomical reconstruction (TAR) technique [11]. For 3D cognitive RARP the surgeon had the chance to consult on-demand the

HA3D™ model during the intervention, whilst for AR-RARP the intervention was executed with the 3D overlapped images, as previously published [7,8] (Figure 1b,c). In particular, images obtained by the endoscopic view were mixed with the 3D virtual model thanks to vMix software (https://www.vmix.com); the overlapping of the 3D models over the real anatomy was performed manually, using our previously developed *p-Viewer* platform, by a surgical assistant with the support of a 3D professional mouse. Finally, the obtained merged images were sent back to the Da Vinci remote console using the Tile-Pro.

With the aim to maximally preserve the nervous fibers in the Neurovascular bundles (NVBs), an antegrade nerve sparing (NS) RARP adapted to patient's preoperative features was performed.

2.4 **Control group**

The Control group consisted of patients with a pre-operative mpMRI who underwent RARP with TAR technique in the same study period. All patients were treated by the same surgeon (FP), who already reached his learning curve plateau (more than 200 cases/year over the last five years), without the fruition of 3D models due to issues in the 3D models production or absence of bioengineer's assistance. Surgeons had the chance to consult mp-MRI images during the intervention.

In order to optimize the nature of comparison with the control group (no 3D RARP), we relied on 1:4 propensity score (PS) matching according to the nearest neighbor [12]. The 1:4 PS-matched cohorts (3D vs no 3D RARP) were balanced according to age, BMI, PSA, GS, DRE, prostate volume, Pi-Rads score, presence of ECE or SVI.

2.5 **Data collection**

Collected data from the two groups included preoperative variables in terms of demographic, radiological and pathological features.

Intraoperative variables were also recorded: in particular the rate of full vs intermediate vs standard NS procedures (according to Pasadena Consensus classification [13]) was collected. Full NS means bilateral intrafascial; partial/intermediate NS refers to interfascial/intrafascial or interfascial/interfascial; and standard NS is interfascial/extrafascial or extrafascial/extrafascial.

Then, postoperative variables such as catheterization time, hospitalization time, and complication rates (according to Clavien–Dindo classification [14]) were evaluated.

Pathological variables were analyzed, and clinically significant positive surgical margins, defined as multifocal or ≥ 3 mms [15], were evaluated.

Potency recovery was recorded using the International Index of Erectile Function questionnaire (score ≥17 means "valid erection") [16]; urinary continence recovery was stated if the patients did not use any pads or if they used one safety pad/day at catheter removal or at 1, 3, 6 and 12 months after RARP. Short-term oncological follow-up was evaluated at a minimum of 12 months, comparing BCR between the 3D and no-3D control group. BCR was denoted as (i) any postoperative cancer treatment, or (ii) PSA level >0.2 ng/mL with a single repeated measurement for confirmation.

2.6 **Statistical analysis**

Descriptive statistics included frequencies and proportions for continuous and categorical variables, respectively. The statistical significance of differences in proportions was evaluated with chi-square tests. Statistical analyses consisted of five analytical steps.

First, we tabulated rates of NS approach according to 3D technology availability. Second, we tabulated PSM rates according to the type of NS between 3D (cognitive or AR) vs. no 3D technology availability. Third, we fitted MLR models predicting the presence of PSM. Covariates consisted of 3D technology availability, presence of ECE, SVI and high D'Amico risk group. Fourth, we tried to identify a specific subgroup of patients in whom 3D technology availability could maximize the protective effect towards PSM. To reach this goal, we fitted four additional MLR models in the following subgroup of patients: patients with ECE at mpMRI, D'Amico high risk category patients, positive DRE and pT3 patients.

The concordance between the index lesion location and the PSM location was evaluated with Cohen's Kappa coefficient.

Finally, Kaplan-Meier (KM) calculation was used to estimate BCR rates at 12 months according to the availability of 3D technology. The same analysis was also fitted in the subgroup of patients with ECE and with pT3 stage.

All statistical tests were two-sided with a level of significance set at $p < 0.05$. Analyses were performed using the R software for statistical computing and graphics (version 3.4.1; http://www.r-project.org/).

3. RESULTS

3.1 Demographics, perioperative and pathological findings

The comparison between 3D and no-3D RARP prior to any matching relied on 160 3D (11%) and 1289 no 3D RARP patients (89%). Specifically, regarding 3D RARP patients, 56 underwent cognitive RARP and 104 AR 3D RARP. After the PS-matching between each 3D RARP patient with up to 4 no-3D RARP patients, 160 3D and 640 no-3D patients were available for the purpose of subsequent analyses and no statistically significant differences remained between both groups in terms of demographic, radiological and biopsy pathological variables (Supplementary materials 1). Focusing on intraoperative variables, a more conservative NS approach (higher rate of full NS) was registered in 3D group (full NS 20.6% vs 12.7%; intermediate NS 38.1% vs 38.0%; standard NS 41.2% vs 49.2%; p= 0.02) (Figure 2a). Postoperative complication rates were comparable (5.6% vs. 4.8%, for 3D vs. Control group patients; p=0.9) (Table 1). Final pathological analysis showed no significant difference between the tumor characteristics in terms of pT of the two Groups (p= 0.051).

3.2 Primary endpoint: PSM evaluation

3D Group patients (regardless of the type of technology used, cognitive or AR) had lower PSM rates (25 vs. 35.1%, p=0.01), compared to their no-3D counterpart. In both groups a good concordance between index lesion location (visualized on 3D models or mp-MRI images) and PSM was recorded (k= 0.89 and k=0.86 in 3D and no 3D group respectively). Only in 5 (3.1%) and 28 (4.3%) cases in 3D and no-3D group respectively (p= 0.64) pathological ECE was found contralaterally to MRI findings. The occurrence of PSM at the level of the index lesion was registered in 43.2% vs 47.0% of the cases in 3D and no-3D Group respectively (p=0.66).
After performing a stratification according to the NS approach, no differences in terms of PSMr were recorded in full and intermediate group (p= 0.87 and p= 0.21 respectively), whilst a significant decrease of PSMr in favour of 3D Group was recorded in standard NS population (p=0.03) (Figure 2b). Moreover, we observed that a higher rate of full NS was performed homolaterally to the index lesion in the 3D group compared to the Control Group (37% vs 14% at right side, p<0.001; 19.6% vs 13% at left side; p=0.06).

Finally, at MLR models the availability of 3D technology (OR: 0.5, CI:0.3-0.8, p= 0.005) and the absence of extracapsular extension (ECE, OR: 0.6, CI:0.4-0.9, p=0.004) at mpMRI were independent predictors of lower PSM rates (Supplementary materials 2 and 3). Moreover, considering the different way of 3D technology fruition, the use of AR revealed to be more protective against PSM than the "cognitive" approach (p= 0.004 vs p= 0.03).
For sensitivity analyses, the MLR models fitted in the specific subgroups of patients with ECE, D'Amico high risk category, positive DRE or pT3 disease, revealing that the availability of 3D model is a significant protective factor for PSM in patients with ECE or pT3 (Supplementary material 4)

3.3 Secondary endpoint: functional outcomes and BCR

Focusing on continence and potency recovery, no differences were found between the two groups at every time of evaluation, as shown in Supplementary material 5. Kaplan-Meier plots revealed no differences in terms of BCR at 12 months of FU in 3D and no-3D group, both in the overall population (p=0.07), as well as in the pT3 (p=0.16) and ECE+ patients (p=0.18) (Figure 2c,d,e).

4. DISCUSSION

Herein we reported the largest series of PCa patients who underwent RARP with the assistance of 3D models' reconstruction.

Our findings revealed that the availability of 3D models before and during the surgical procedure is significantly related to lower postoperative PSMr (p= 0.01). In particular, the MLR models revealed that availability of 3D technology (OR: 0.5, CI:0.3-0.8, p= 0.005) and the absence of extracapsular extension at mpMRI (ECE, OR: 0.6, CI:0.4-0.9, p=0.004) were independent predictors of lower PSM rates. As recently reported by Martini et al. [15] the occurrence of PSM after surgery is related to a higher risk of developing metastasis; therefore the possibility to visualize the tumor burden three dimensionally with a subsequent reduction of PSM can potentially have an impact on oncological outcomes.

Moreover, we observed that in the 3D group a more conservative NS approach was performed (p= 0.02) without affecting the PSMr in full and intermediate NS group (p= 0.87 and p= 0.21 respectively), whilst a significant decrease was observed in standard NS population (p= 0.03). These findings are particularly noteworthy in the current precision cancer surgery era [1]: the possibility to interact with a patient's specific 3D model can help the surgeon to have a better perception of the tumour location and its relationship with NVBs [6, 9] with a subsequently more tailored NS approach.

In fact, nowadays, the new generation of 3D models, created with professional softwares authorized for medical use thanks to a collaboration between urologists, radiologists and bioengineers, have already proven their accuracy in localized cancer lesions, in accordance with final pathology findings [7,8].

Trying to focus on 3D technology, in our recently published study [9] we already demonstrated that, particularly during planning and navigation, surgeons preferred the use of 3D virtual models, avoiding the necessity to have a physical 3D printed model, with a significant money saving.

However, notwithstanding the increasing diffusion of 3D technology in PCa surgery, the experiences evaluating the role of 3D virtual models in a cognitive manner, remain few [17]. In a phase 1 feasibility study, Kratiras et al. [18] introduced a surgical navigation system during RARP with the use of a tablet. Thanks to a dedicated touch-screen computer, a magnetic field generator, position sensors and a tracking system, the 3D image could follow the prostate's intraoperative

movements, highlighting malignancy's location and helping the surgeon throughout the procedure.

Focusing on AR technology, it represents the maximal expression of the 3D image guided surgery, perfectly merging with the robotic platform. In fact, following the pioneering experiences during laparoscopic prostatectomy in the first decade of the XXIst century [19-22], our group developed an AR platform for robotic prostatectomy. The 3D virtual prostate model can be overlapped to the in-vivo endoscopic view in real time, thanks to an expert assistant using a 3D professional mouse [7,8]. Moreover, to overcome the need of continuous human assistance (and potential intrinsic error), we started to test an automatic image overlapping software, with promising results [23]. In particular, artificial intelligence driven convolutional neuronal networks were used to automatically identify the anatomical landmarks and to anchor the 3D virtual models to the real anatomy images [24].

It's interesting to denote that, even if both 3D modelling visualization modalities led to an advantage in terms of PSMr compared to standard approach, the sub-analysis with MLR models revealed that patients treated with AR procedures had a more significant reduction of PSMr compared to the "cognitive" group.

From our point of view, these findings are not surprising: AR technology represents indeed the natural evolution of this kind of 3D image guided surgery, and even if nowadays we are still in the field of clinical research, its benefits in terms of surgical accuracy are astonishing.

In addition, in order to further improve the safety of 3D AR guided NS, intraoperative frozen section can be analysed to verify the radicality of the resection [25, 26].

Then, aiming to identify a specific subgroup of patients who could maximally benefit from the use of 3D technology, we fitted four additional MLR models. Our sensitivity analyses revealed that patients with ECE or pT3 PCa were the most affected cohort. We think that the identification of a specific cohort benefitting the most from the use of 3D models could be useful in order to better manage the available resources, both from a technological and economic point of view.

Lastly, focusing on oncological outcomes in terms of BCR, even though a one year follow-up is too short to assess any final consideration, KM analysis did not reveal any differences between the two groups, notwithstanding the more conservative NS approach of the 3D Group. On the contrary, concerning continence and potency recovery rates, a slightly positive trend in favour of 3D group was recorded: further studies on a larger population will allow to highlight the potential advantages of 3D models' use. However, we might speculate that if the availability of 3D models

determines the use of a more conservative NS approach without increasing the risk of PSM or BCR (Figure 2), we will expect a higher rate of sexually potent patients in the 3D cohort thanks to a higher amount of NVBs spared and a lower probability of postoperative treatment such as radiotherapy or hormonal therapy, supporting the feasibility of NS procedures even in cases of high risk tumour [27].

Notwithstanding the above-mentioned findings, our study is not devoid of limitations. Firstly, this study has retrospective approach and even if matched, control group could have several selection biases. Secondarily, 3D models' accuracy is MRI-quality and resolution dependent. In fact, in case of focal ECE they could therefore be unprecise and their impact on the decrease of PSM is not assessable; thirdly, up to now prostate and neoplasm segmentation were partially performed manually: an experienced urologist and radiologist were necessary to complete the segmentation process. Lastly, in AR population, the entire overlap process is operator dependent. At last, the absence of randomization and the short follow-up limit the power of our results.

In the next future, a randomized controlled trial with IRB approval is necessary to overcome these methodological limitations. Moreover, under a technical point of view, the breakthrough advent of artificial intelligence guided surgery will allow to perform "humanless" automatic AR procedures [28, 29].

5. CONCLUSION

Our findings suggest that the chance to have at surgeon's disposal a patient specific 3D model during the intervention allows to have expand the indication to NS surgery, limiting, ath the same time, the occurrence of postoperative PSM. In particular, patients with ECE at mpMRI or pT3 disease can obtain the greatest advantages. Moreover, AR technology can lead to a further improvement of oncological safety, thanks to its real-time navigation.

AUTHORS' CONTRIBUTION

Protocol/project development: E. Checcucci, D. Amparore, A. Pecoraro, F. Porpiglia

Data collection or management: S. De Cillis, S. Granato, M. Sica, A. Piana, P. Verri

Data analysis: A. Pecoraro

Manuscript writing/editing: E. Checcucci, G. Volpi, A. Pecoraro

Supervision: C. Fiori, M. Di Dio, M. Manfredi, P. Piazzolla, E. Vezzetti, F. Porpiglia

DISCOLOSURE OR CONFLICT OF INTEREST:

All the authors have nothing to disclose.

RESEARCH INVOLVING HUMAN PARTICIPANTS AND/OR ANIMALS

None

INFORMED CONSENT

None

REFERENCES:

1. Checcucci E, Amparore D, De Luca S, Autorino R, Fiori C, Porpiglia F. Precision prostate cancer surgery: an overview of new technologies and techniques. Minerva Urol Nefrol. 2019 Oct;71(5):487-501. doi: 10.23736/S0393-2249.19.03365-4. Epub 2019 Jan 28. PMID: 30700084.
2. Lee S, Kim KB, Jo JK, Ho JN, Oh JJ, Jeong SJ, Hong SK, Byun SS, Choe G, Lee SE. Prognostic Value of Focal Positive Surgical Margins After Radical Prostatectomy. Clin Genitourin Cancer. 2016 Aug;14(4):e313-9. doi: 10.1016/j.clgc.2015.12.013. Epub 2015 Dec 29. PMID: 27130538.
3. Dinneen E, Haider A, Grierson J, Freeman A, Oxley J, Briggs T, Nathan S, Williams NR, Brew-Graves C, Persad R, Aning J, Jamieson C, Ratynska M, Ben-Salha I, Ball R, Clow R, Allen C, Heffernan-Ho D, Kelly J, Shaw G. NeuroSAFE frozen section during robot-assisted radical prostatectomy (RARP): Peri-operative and Histopathological Outcomes from the NeuroSAFE PROOF Feasibility Randomised Controlled Trial. BJU Int. 2020 Sep 27. doi: 10.1111/bju.15256. Epub ahead of print. PMID: 32985121.
4. Rocco B, Sighinolfi MC, Cimadamore A, Reggiani Bonetti L, Bertoni L, Puliatti S, Eissa A, Spandri V, Azzoni P, Dinneen E, Shaw G, Nathan S, Micali S, Bianchi G, Maiorana A, Pellacani G, Montironi R. Digital frozen section of the prostate surface during radical prostatectomy: a novel approach to evaluate surgical margins. BJU Int. 2020 Sep;126(3):336-338. doi: 10.1111/bju.15108. PMID: 32401370.
5. Russo F, Manfredi M, Panebianco V, Armando E, De Luca S, Mazzetti S, Giannini V, Mele F, Bollito E, Appendino E, Regge D, Porpiglia F. Radiological Wheeler staging system: a retrospective cohort analysis to improve the local staging of prostate cancer with multiparametric MRI. Minerva Urol Nefrol. 2019 Jun;71(3):264-272. doi: 10.23736/S0393-2249.19.03248-X. Epub 2019 Jan 17. PMID: 30654601.
6. Porpiglia F, Bertolo R, Checcucci E, Amparore D, Autorino R, Dasgupta P, Wiklund P, Tewari A, Liatsikos E, Fiori C; ESUT Research Group. Development and validation of 3D printed virtual models for robot-assisted radical prostatectomy and partial nephrectomy: urologists' and patients' perception. World J Urol. 2018 Feb;36(2):201-207. doi: 10.1007/s00345-017-2126-1. Epub 2017 Nov 10. PMID: 29127451.
7. Porpiglia F, Checcucci E, Amparore D, Manfredi M, Massa F, Piazzolla P, Manfrin D, Piana A, Tota D, Bollito E, Fiori C. Three-dimensional Elastic Augmented-reality Robot-assisted

Radical Prostatectomy Using Hyperaccuracy Three-dimensional Reconstruction Technology: A Step Further in the Identification of Capsular Involvement. Eur Urol. 2019 Oct;76(4):505-514. doi: 10.1016/j.eururo.2019.03.037. Epub 2019 Apr 9. PMID: 30979636.

8. Porpiglia F, Checcucci E, Amparore D, Autorino R, Piana A, Bellin A, Piazzolla P, Massa F, Bollito E, Gned D, De Pascale A, Fiori C. Augmented-reality robot-assisted radical prostatectomy using hyper-accuracy three-dimensional reconstruction (HA3D™) technology: a radiological and pathological study. BJU Int. 2019 May;123(5):834-845. doi: 10.1111/bju.14549. Epub 2018 Oct 19. PMID: 30246936.
9. Amparore D, Pecoraro A, Checcucci E, et al 3D imaging technologies in minimally-invasive kidney and prostate cancer surgery: which is the urologists' perception? Minerva Urol Nefrol. 2021 in press
10. Russo F, Regge D, Armando E, Giannini V, Vignati A, Mazzetti S, Manfredi M, Bollito E, Correale L, Porpiglia F. Detection of prostate cancer index lesions with multiparametric magnetic resonance imaging (mp-MRI) using whole-mount histological sections as the reference standard. BJU Int. 2016 Jul;118(1):84-94. doi: 10.1111/bju.13234. Epub 2015 Aug 24. PMID: 26198404.
11. Porpiglia F, Bertolo R, Manfredi M, De Luca S, Checcucci E, Morra I, Passera R, Fiori C. Total Anatomical Reconstruction During Robot-assisted Radical Prostatectomy: Implications on Early Recovery of Urinary Continence. Eur Urol. 2016 Mar;69(3):485-95. doi: 10.1016/j.eururo.2015.08.005. Epub 2015 Aug 19. PMID: 26297603.
12. Austin PC. An Introduction to Propensity Score Methods for Reducing the Effects of Confounding in Observational Studies. Multivariate Behav Res. 2011;46(3):399-424. doi:10.1080/00273171.2011.568786
13. Montorsi F, Wilson TG, Rosen RC, Ahlering TE, Artibani W, Carroll PR, Costello A, Eastham JA, Ficarra V, Guazzoni G, Menon M, Novara G, Patel VR, Stolzenburg JU, Van der Poel H, Van Poppel H, Mottrie A; Pasadena Consensus Panel. Best practices in robot-assisted radical prostatectomy: recommendations of the Pasadena Consensus Panel. Eur Urol. 2012 Sep;62(3):368-81. doi: 10.1016/j.eururo.2012.05.057. Epub 2012 Jun 7. PMID: 22763081.
14. Dindo D, Demartines N, Clavien PA. Classification of surgical complications: a new proposal with evaluation in a cohort of 6336 patients and results of a survey. Ann Surg. 2004 Aug;240(2):205-13. doi: 10.1097/01.sla.0000133083.54934.ae. PMID: 15273542; PMCID: PMC1360123.

15. Martini A, Gandaglia G, Fossati N, Scuderi S, Bravi CA, Mazzone E, Stabile A, Scarcella S, Robesti D, Barletta F, Cucchiara V, Mirone V, Montorsi F, Briganti A. Defining Clinically Meaningful Positive Surgical Margins in Patients Undergoing Radical Prostatectomy for Localised Prostate Cancer. Eur Urol Oncol. 2019 Apr 4:S2588-9311(19)30039-2. doi: 10.1016/j.euo.2019.03.006. Epub ahead of print. PMID: 31411971.
16. Rosen RC, Riley A, Wagner G, Osterloh IH, Kirkpatrick J, Mishra A. The international index of erectile function (IIEF): a multidimensional scale for assessment of erectile dysfunction. Urology. 1997 Jun;49(6):822-30. doi: 10.1016/s0090-4295(97)00238-0. PMID: 9187685.
17. Wang S, Frisbie J, Keepers Z, Bolten Z, Hevaganinge A, Boctor E, Leonard S, Tokuda J, Krieger A, Siddiqui MM. The Use of Three-dimensional Visualization Techniques for Prostate Procedures: A Systematic Review. Eur Urol Focus. 2020 Aug 29:S2405-4569(20)30215-7. doi: 10.1016/j.euf.2020.08.002. Epub ahead of print. PMID: 32873515.
18. Kratiras Z, Gavazzi A, Belba A, Willis B, Chew S, Allen C, Amoroso P, Dasgupta P. Phase I study of a new tablet-based image guided surgical system in robot-assisted radical prostatectomy. Minerva Urol Nefrol. 2019 Feb;71(1):92-95. doi: 10.23736/S0393-2249.18.03250-2. Epub 2018 Nov 7. PMID: 30421593.
19. Ukimura O, Gill IS. Imaging-assisted endoscopic surgery: Cleveland Clinic experience. J Endourol. 2008 Apr;22(4):803-10. doi: 10.1089/end.2007.9823. PMID: 18366316.
20. Teber D, Simpfendörfer T, Guven S, Baumhauer M, Gözen AS, Rassweiler J. In-vitro evaluation of a soft-tissue navigation system for laparoscopic prostatectomy. J Endourol. 2010 Sep;24(9):1487-91. doi: 10.1089/end.2009.0289. PMID: 20726787.
21. Simpfendörfer T, Baumhauer M, Müller M, Gutt CN, Meinzer HP, Rassweiler JJ, Guven S, Teber D. Augmented reality visualization during laparoscopic radical prostatectomy. J Endourol. 2011 Dec;25(12):1841-5. doi: 10.1089/end.2010.0724. Epub 2011 Oct 4. PMID: 21970336.
22. Lanchon C, Custillon G, Moreau-Gaudry A, Descotes JL, Long JA, Fiard G, Voros S. Augmented Reality Using Transurethral Ultrasound for Laparoscopic Radical Prostatectomy: Preclinical Evaluation. J Urol. 2016 Jul;196(1):244-50. doi: 10.1016/j.juro.2016.01.094. Epub 2016 Jan 25. PMID: 26820551.
23. Amparore D, Checcucci E, Fiori C, Porpiglia F. Reply to Mengda Zhang and Long Wang's Letter to the Editor re: Francesco Porpiglia, Enrico Checcucci, Daniele Amparore, et al. Three-dimensional Augmented Reality Robot-assisted Partial Nephrectomy in Case of

Complex Tumours (PADUA ≥ 10): A New Intraoperative Tool Overcoming the Ultrasound Guidance. Eur Urol. In press. Eur Urol. 2020 Jun;77(6):e163-e164. doi: 10.1016/j.eururo.2020.03.038. Epub 2020 Apr 9. PMID: 32279902.

24. F. Porpiglia, E. Checcucci, D. Amparore, P. Piazzolla, M. Manfredi, A. Pecoraro, S. De Cillis, A. Piana, G. Volpi, F. Piramide, P. Alessio, S. Granato, E. Vezzetti, C. Fiori, P1100 - Artificial intelligence guided 3D automatic augmented-reality images allow to identify the extracapsular extension on neurovascular bundles during robotic prostatectomy, European Urology, Volume 79, Supplement 1, 2021, Page S1560, ISSN 0302-2838, https://doi.org/10.1016/S0302-2838(21)01471-8.
25. Bianchi L, Chessa F, Angiolini A, Cercenelli L, Lodi S, Bortolani B, Molinaroli E, Casablanca C, Droghetti M, Gaudiano C, Mottaran A, Porreca A, Golfieri R, Romagnoli D, Giunchi F, Fiorentino M, Piazza P, Puliatti S, Diciotti S, Marcelli E, Mottrie A, Schiavina R. The Use of Augmented Reality to Guide the Intraoperative Frozen Section During Robot-assisted Radical Prostatectomy. Eur Urol. 2021 Jul 28:S0302-2838(21)01861-3. doi: 10.1016/j.eururo.2021.06.020. Epub ahead of print. PMID: 34332759.
26. Schiavina R, Bianchi L, Lodi S, Cercenelli L, Chessa F, Bortolani B, Gaudiano C, Casablanca C, Droghetti M, Porreca A, Romagnoli D, Golfieri R, Giunchi F, Fiorentino M, Marcelli E, Diciotti S, Brunocilla E. Real-time Augmented Reality Three-dimensional Guided Robotic Radical Prostatectomy: Preliminary Experience and Evaluation of the Impact on Surgical Planning. Eur Urol Focus. 2020 Aug 31:S2405-4569(20)30217-0. doi: 10.1016/j.euf.2020.08.004. Epub ahead of print. PMID: 32883625.
27. Morozov A, Barret E, Veneziano D, Grigoryan V, Salomon G, Fokin I, Taratkin M, Poddubskaya E, Gomez Rivas J, Puliatti S, Okhunov Z, Cacciamani GE, Checcucci E, Marenco Jiménez JL, Enikeev D; in collaboration with ESUT-YAUWP Group. A systematic review of nerve-sparing surgery for high-risk prostate cancer. Minerva Urol Nefrol. 2021 Jan 13. doi: 10.23736/S0393-2249.20.04178-8. Epub ahead of print. PMID: 33439578.
28. Checcucci E, Autorino R, Cacciamani GE, Amparore D, De Cillis S, Piana A, Piazzolla P, Vezzetti E, Fiori C, Veneziano D, Tewari A, Dasgupta P, Hung A, Gill I, Porpiglia F; Uro-technology and SoMe Working Group of the Young Academic Urologists Working Party of the European Association of Urology. Artificial intelligence and neural networks in urology: current clinical applications. Minerva Urol Nefrol. 2020 Feb;72(1):49-57. doi: 10.23736/S0393-2249.19.03613-0. Epub 2019 Dec 12. PMID: 31833725.

29. Checcucci E, De Cillis S, Granato S, Chang P, Afyouni AS, Okhunov Z; Uro-technology and SoMe Working Group of the Young Academic Urologists Working Party of the European Association of Urology. Applications of neural networks in urology: a systematic review. Curr Opin Urol. 2020 Nov;30(6):788-807. doi: 10.1097/MOU.0000000000000814. PMID: 32881726.

FIGURE LEGENDS:

Figure 1: a) Hyper-Accuracy 3D model (HA3D®) of the prostate (courtesy of MEDICS Srl (www.medics3d.com); b) 3D Cognitive RARP: the surgeon had the possibility to consult the 3D model on-demand during the intervention; c) 3D AR RARP: the 3D model was overlapped to in-vivo anatomy and visualized inside robotic console monitor

Figure 2: a) Different degree of nerve sparing according to the different surgical approach (3D Group vs no3D Group); b) Rate of PSM according to the degree of nerve-sparing and to 3D technology availability; Kaplan Meier plots depicting biochemical recurrence (BCR) at 12 months within the overall population (c), pT3 stage patients (d), and ECE patients (e)

Figure

Click here to access/download;Figure;Figure 1_n.jpg

Figure

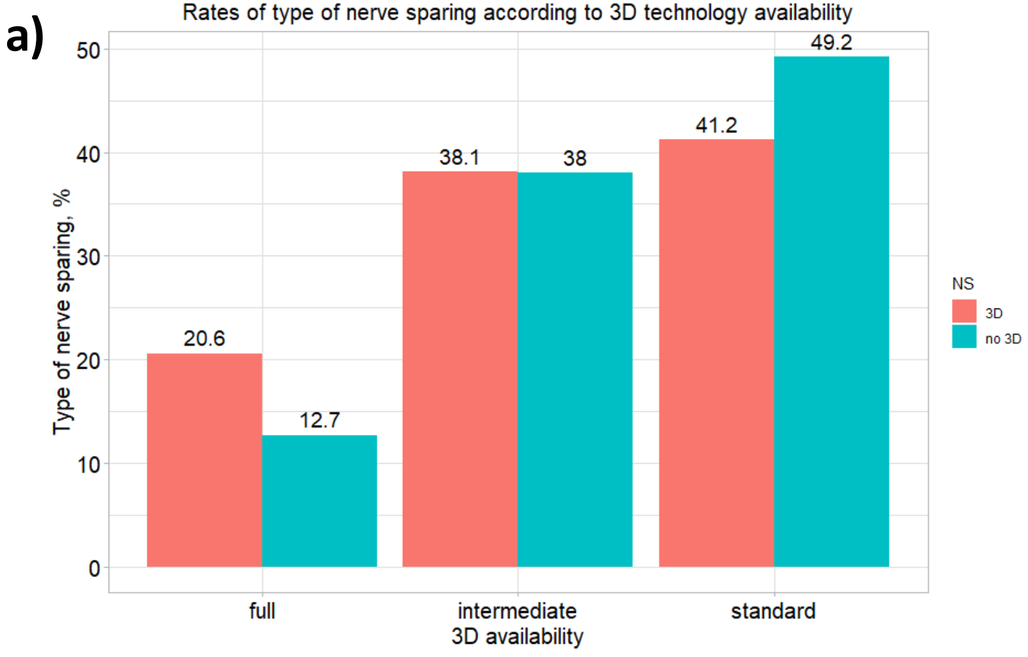

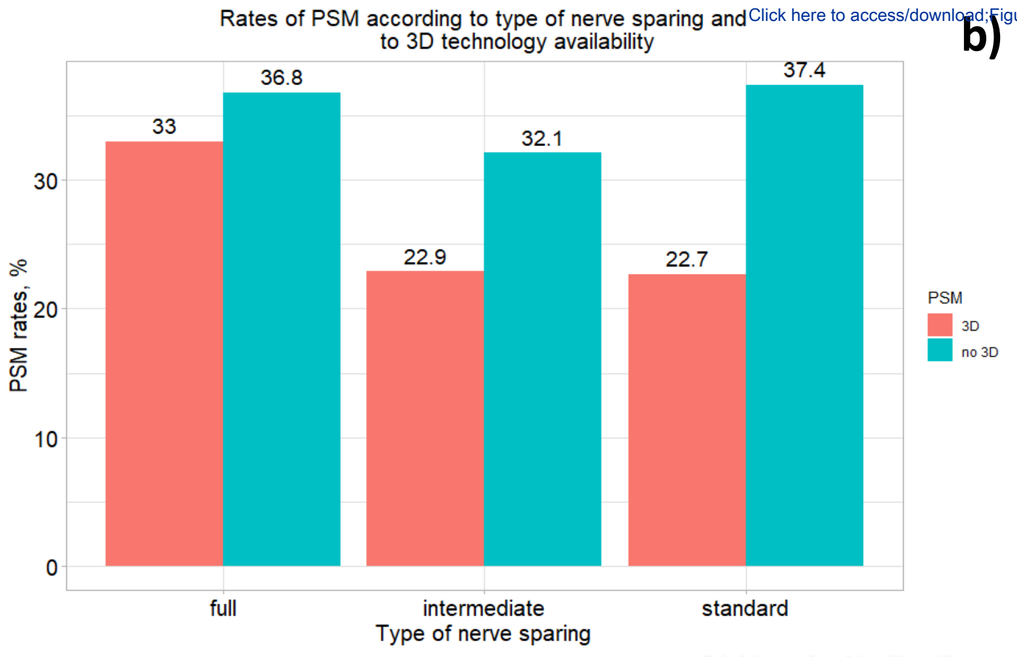

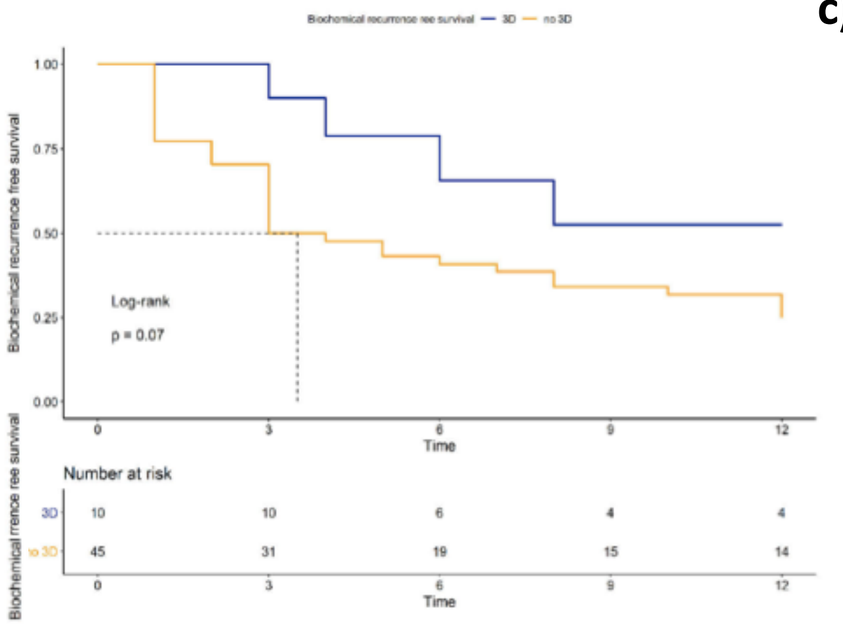

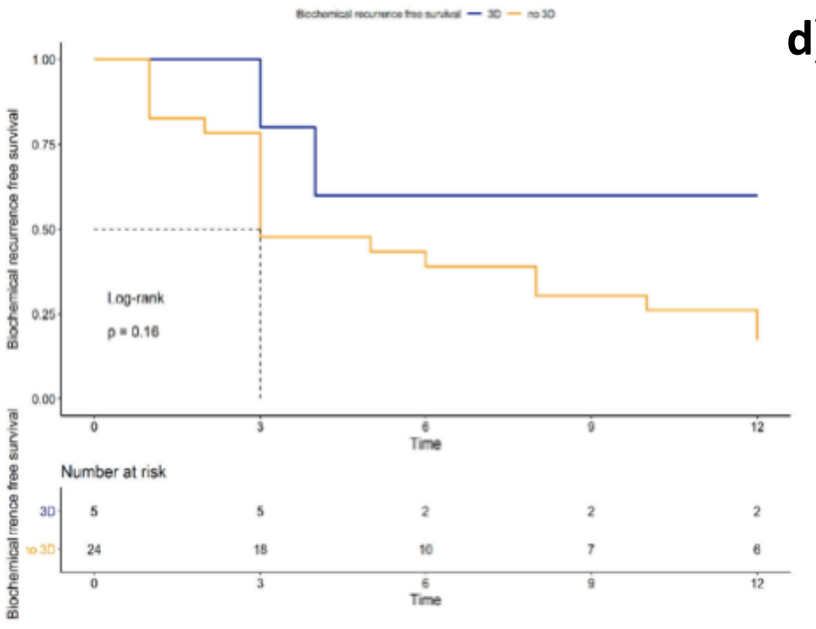

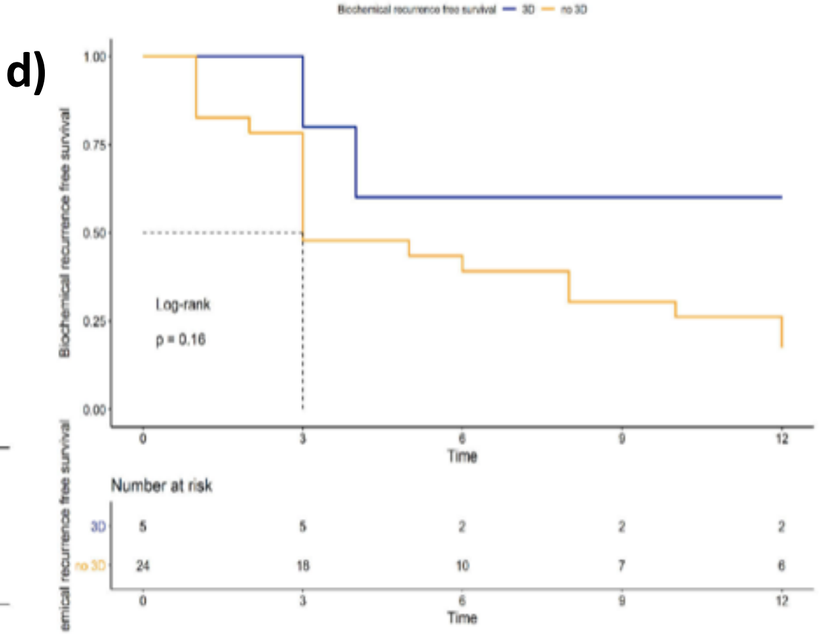

e)

		Overall	3D	no 3D	p-value
Operative time	Mean (SD)	117.6 (1.127)	113 (2.381)	118 (1.273)	0.07
Nerve-Sparing	full	114 (14.2)	33 (20.6)	81 (12.7)	Full: 0.01 Intermediate: 0.9 Standard: 0.06 Overall: 0.02
	intermediate	304 (38)	61 (38.1)	243 (38)	
	standard	381 (47.6)	66 (41.2)	315 (49.2)	
Postoperative complication	N (%)	40 (5)	9 (5.6)	31 (4.8)	0.9
pT	pT2	337 (42.1)	64 (38.8)	273 (42.7)	0.051
	pT3a	368 (46.0)	81 (50.6)	287 (43.4)	
	pT3b	93 (11.6)	15 (9.4)	78 (12.2)	
PSM: - total - pT2 - pT3	N (%)	 265 (33.1) 87 (25.8) 178 (38.6)	 40 (25) 13 (20.3) 27 (28,1)	 225 (35.1) 74 (27.1) 151 (41.3)	0.01
PSM location: - posterior/posterolateral - anterior apex - posterior apex	N (%)	 108 (40.7) 86 (32.4) 71 (26.8)	 17 (42.5) 13 (32.5) 10 (25)	 91 (40.4) 73 (32.4) 61 (27.2)	0.07

Table 1: Postoperative variables (PSM: positive surgical margin; SD: standard deviation)